Abdominal Radiology (2023) 48:282–290
https://doi.org/10.1007/s00261-022-03687-y

TECHNICAL

Accelerated T2-weighted MRI of the liver at 3 T using a single-shot technique with deep learning-based image reconstruction: impact on the image quality and lesion detection

Luke A. Ginocchio[1] · Paul N. Smereka[1] · Angela Tong[1] · Vinay Prabhu[1] · Dominik Nickel[2] · Simon Arberet[3] · Hersh Chandarana[1] · Krishna P. Shanbhogue[1]

Received: 26 January 2022 / Revised: 15 September 2022 / Accepted: 16 September 2022 / Published online: 28 September 2022
© The Author(s), under exclusive licence to Springer Science+Business Media, LLC, part of Springer Nature 2022

Abstract

Purpose Fat-suppressed T2-weighted imaging (T2-FS) requires a long scan time and can be wrought with motion artifacts, urging the development of a shorter and more motion robust sequence. We compare the image quality of a single-shot T2-weighted MRI prototype with deep-learning-based image reconstruction (DL HASTE-FS) with a standard T2-FS sequence for 3 T liver MRI.

Methods 41 consecutive patients with 3 T abdominal MRI examinations including standard T2-FS and DL HASTE-FS, between 5/6/2020 and 11/23/2020, comprised the study cohort. Three radiologists independently reviewed images using a 5-point Likert scale for artifact and image quality measures, while also assessing for liver lesions.

Results DL HASTE-FS acquisition time was 54.93 ± 16.69, significantly ($p < .001$) shorter than standard T2-FS (114.00 ± 32.98 s). DL HASTE-FS received significantly higher scores for sharpness of liver margin (4.3 vs 3.3; $p < .001$), hepatic vessel margin (4.2 vs 3.3; $p < .001$), pancreatic duct margin (4.0 vs 1.9; $p < .001$); in-plane (4.0 vs 3.2; $p < .001$) and through-plane (3.9 vs 3.4; $p < .001$) motion artifacts; other ghosting artifacts (4.3 vs 2.9; $p < .001$); and overall image

✉ Luke A. Ginocchio
  Luke.Ginocchio@nyulangone.org

  Paul N. Smereka
  paul.smereka@nyulangone.org

  Angela Tong
  angela.tong@nyulangone.org

  Vinay Prabhu
  vinay.prabhu@nyulangone.org

  Dominik Nickel
  marcel.nickel@siemens-healthineers.com

  Simon Arberet
  simon.arberet@siemens-healthineers.com

  Hersh Chandarana
  hersh.chandarana@nyulangone.org

  Krishna P. Shanbhogue
  krishna.shanbhogue@nyulangone.org

[1] Department of Radiology, NYU Grossman School of Medicine, NYU Langone Health, 660 First Avenue, 3rd Floor, New York, NY 10016, USA

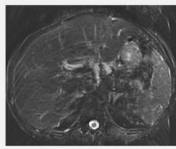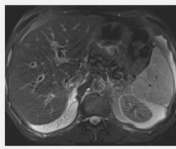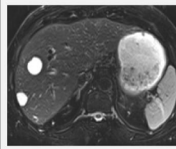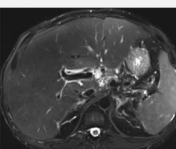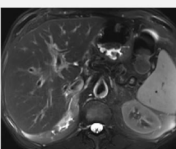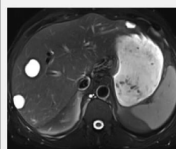[2] MR Applications Predevelopment, Siemens Healthcare GmbH, 91052 Erlangen, Germany

[3] Digital Technology and Innovation, Siemens Healthineers, Princeton, NJ 08540, USA

quality (4.0 vs 2.9; $p < .001$), in addition to receiving a higher score for homogeneity of fat suppression (3.7 vs 3.4; $p = .04$) and liver-fat contrast ($p = .03$). For liver lesions, DL HASTE-FS received significantly higher scores for sharpness of lesion margin (4.4 vs 3.7; $p = .03$).

Conclusion Novel single-shot T2-weighted MRI with deep-learning-based image reconstruction demonstrated superior image quality compared with the standard T2-FS sequence for 3 T liver MRI, while being acquired in less than half the time.

Graphical abstract

Introduction

Magnet resonance imaging (MRI) of the liver is an increasingly common examination performed for the detection and characterization of focal liver lesions, in addition to the assessment of diffuse liver disease [1–3]. Fat-suppressed T2-weighted imaging (T2-FS) is a critical component of clinical liver MRI, providing a high contrast-to-noise ratio (CNR) to allow for the detection of focal abnormalities [4]. However, traditional T2-FS imaging often requires several minutes of acquisition time to obtain high-quality images, and even with the additional techniques of signal averaging, ordered phase encoding, and gradient moment nulling, and these sequences can be wrought with motion artifacts [5]. More recently, multi-shot 2D fast spin-echo pulse sequences (T2 FSE) with frequency-selective fat suppression have been used for sequence acquisition [6–8]. In addition to allowing for quicker acquisition times, T2 FSE techniques provide greater differences in signal intensity between solid and nonsolid lesions than on conventional SE images, likely as a result of greater magnetization-transfer contrast [9]. Even with these reductions in acquisition time, current T2 FSE protocols employ multi-shot acquisitions susceptible to respiratory motion, prompting the need for techniques, such as multi-breath-hold acquisitions, prospective respiratory triggering (RT), or navigator-based triggering (PACE) to acquire diagnostically acceptable images [10, 11]. Despite these additional steps, T2-FS images remain motion sensitive with associated low-quality images, diagnostically unacceptable blurring, and motion artifacts, often prompting repeat acquisitions, reportedly occurring as frequently as 54.7% at one institution [12].

Several methods have been explored to improve image quality, including 3D fast spin-echo pulse sequences (SPACE [Siemens Healthcare, Erlangen, Germany],

CUBE [General Electric Healthcare, Milwaukee, WI, USA], VISTA [Philips Healthcare, Best, the Netherlands]), and periodically rotated overlapping parallel lines with enhanced reconstruction (PROPELLER [General Electric Healthcare, Milwaukee, WI, USA], BLADE [Siemens Healthcare, Erlangen, Germany], MultiVane [Philips Healthcare, Best, the Netherlands]), but at the cost of increased overall acquisition times [13, 14].

Single-shot T2-weighted imaging has also been suggested as an approach for reducing motion artifacts, given that these sequences have faster acquisition times and are, at baseline, more motion robust. However, traditional single-shot techniques have lower image contrast than T2 FSE, owing to the need to balance echo time and duration during the acquisition of single-shot images, given that longer echo train durations lead to increased T2 blurring. To attain the desired echo time, single-shot FSE sequences often use short echo spacings and partial Fourier acquisition, resulting in decreased scan times and motion artifacts, but at the expense of decreased spatial resolution, signal-to-noise ratio (SNR), and focal lesion conspicuity [15–18]. In addition, these single-shot techniques often lack fat suppression, which limits the detection and characterization of focal lesions due to increased ghosting artifacts from high signal fat and decreased liver-to-lesion contrast [19–21]. However, the addition of fat suppression techniques may result in inhomogeneous signal suppression near the body-array coil and increases overall scan time [20]. Consequently, there remains a need for the development of a shorter and more motion robust T2-weighted fat-suppressed MRI sequence for clinical MRI liver imaging.

In order to obtain sufficient image contrast comparable to traditional T2 FSE sequences, a single-shot sequence would require a high acceleration while still maintaining the SNR, which Deep-Learning (DL)-based image reconstructions are able to provide using an iterative procedure consisting of k-space data consistency requirements and image regularization, trained through an optimization process on representative images [22–25]. Recently, a single-shot T2-FS HASTE sequence utilizing deep-learning reconstruction has been employed on clinical 1.5 T MRI liver examinations at one institution, demonstrating decreased imaging times with improved overall image quality [26]. However, these techniques have yet to be implemented on 3 T clinical MRI liver examinations, which carry their own associated challenges due to increased magnetic field strength. Although 3 T examinations demonstrate increased SNR, allowing for improved spatial resolution, in comparison with 1.5 T examinations, they often exhibit exacerbation of artifacts and have specific absorption rate (SAR) limitations [27, 28]. Therefore, we aim to compare the image quality of a single-shot T2-weighted MRI prototype with deep-learning-based

image reconstruction (DL HASTE-FS) with a standard T2-FS sequence for routine clinical liver MRI at 3 T.

Methods

Patients

This prospective HIPAA-compliant study was performed following institutional review board approval with waived informed consent. A total of 41 consecutive patients (male = 27, female = 14, mean age = 58, range = 25–83 years) underwent clinically indicated abdominal MRI examinations at one of our institution's outpatient facilities between May 6, 2020 and November 23, 2020. Clinical indications for the MRIs were as follows: cirrhosis ($n = 18$), focal lesion ($n = 7$), viral hepatitis ($n = 4$), abnormal liver enzymes ($n = 4$), fatty liver disease ($n = 3$), follow-up after liver transplantation ($n = 3$), abdominal pain ($n = 1$), and splenomegaly ($n = 1$).

MR-imaging protocol

MR-imaging studies were performed on clinical 3 T MR imaging systems (MAGNETOM Skyra and Prisma; Siemens Healthcare, Erlangen, Germany), which had the novel prototype DL HASTE-FS sequence available. Traditional fat-suppressed two-dimensional (2D) T2-weighted turbo spin-echo (T2-FS TSE) and DL HASTE-FS sequences were performed as part of the routine 3 T liver MRI protocol. An 18-channel body-array coil and an 8-channel posterior spine coil were used for the imaging study.

Conventional T2-FS sequence acquisition

2D T2-FS acquisition is routinely performed as part of our institution's routine clinical liver MRI protocol and was performed with the following parameters: TR/TE = 3800 ms/105 ms; FA = 132 degrees; spectral-attenuated inversion recovery (SPAIR) was used for fat suppression; FOV = 375×375 mm^2; matrix = 256×205 (matched with DL HASTE-FS acquisition); section thickness = 5 mm (matched with DL HASTE-FS acquisition); resolution (interpolated) = $0.68 \times 0.68 \times 5$ mm^3; receiver bandwidth = 305 Hz/Px; PAT factor = 3; number of axial sections = 40; and number of breath holds = 3 (20 s each).

DL HASTE-FS sequence acquisition

The prototypical DL HASTE-FS sequence is based on the standard HASTE sequence, with the following alterations: During the echo train, no calibration data for the estimation

of coil-sensitivity maps are acquired, but instead the calibration data are acquired in a second echo train following about 50 ms after the image data are acquired, which maintains the motion robustness and even reduces SAR, since lower flip angles can be used for calibration data. In order to avoid crosstalk and magnetization transfer effects, the slice increment of consecutively acquired slices is increased, which obviates artificial delays between the acquisitions of subsequent slices and allows for a repetition time of 500 ms without noticeable change of the image contrast. Conventional parallel imaging sampling patterns are used for the acceleration. Spectral-attenuated inversion recovery (SPAIR) was used for fat suppression [29]. Imaging parameters were as follows: TR/TE = 582 ms/118 ms; FA = 140 degrees; FOV = 375 × 375 mm^2; matrix = 256 × 205 (matched with traditional 2D T2-FS acquisition); section thickness = 5 mm (matched with traditional 2D T2-FS acquisition); resolution (interpolated) = 0.68 × 0.68 × 5 mm^3; receiver bandwidth = 723 Hz/Px; PAT factor = 3; ETL = 64 (for reference, ETL = 82 for conventional HASTE liver imaging); number of axial sections = 30; and number of breath holds = 1. Given that the HASTE sequence is a single-shot acquisition, the term TR is used differently for this type of sequence and refers to the duration between sequentially acquired slices. In addition, the TE provided is truly an "effective TE," since there is no specific time point when it is acquired, instead, data are acquired at multiple TE's and the "effective TE" is placed at the center of K-space to achieve the desired contrast.

DL HASTE-FS reconstruction

DL HASTE-FS sequence reconstruction employs an unrolled iterative reconstruction network which was previously used on 1.5 T MRI liver examinations [26]. This architecture shares some similarities with variational networks introduced previously [22, 24]. Initially, separately acquired calibration data are used to estimate step coil-sensitivity maps. K-space data, bias-field correction, and coil-sensitivity maps are then inserted into the variational network for reconstruction, which uses two types of iterations, both of them with trainable (Nesterov-type) extrapolation steps [30]. No regularization is applied for the first 22 iterations and the network focuses on parallel imaging. Subsequently, a regularization based on residual dense U-net is applied for the following 12 iterations. The empirical finding that initial steps in the variational network focus on signal recovery of missing data near the k-space center allows this approach to perform acquisitions without integrated calibration and using flexible k-space sampling.

Ground-truth images, acquired with parallel imaging, were obtained for the supervised training. Moderate parallel imaging with conventional HASTE protocols was used to acquire training data on volunteers, with the training based on further retrospective down sampling of the acquired data. For example, a typical protocol parameter consisted of a parallel imaging acceleration of 2 in the actual acquisition and an acceleration of 4 in the retrospective down sampling. Approximately 10,000 slices were acquired for training on clinical 1.5 T and 3 T MR scanners (MAGNETOM scanners, Siemens Healthcare, Erlangen, Germany), and the training was implemented in PyTorch and performed on a NVIDIA Tesla V100 (32 GB of memory) GPU.

Subsequently, the trained network was integrated into the scanner reconstruction pipeline by converting into a C + + implemented inference framework. Inference required about 2 s per slice using the given protocol settings for the CPU-only reconstruction on a clinical MRI scanner.

Image analysis

Traditional T2-FS and DL HASTE-FS data were anonymized in Digital Imaging and Communications in Medicine (DICOM) format and randomly assorted. Three board-certified radiologists (with 2, 3, and 4 years of clinical experience in interpretation of MR examinations, respectively) underwent a short training session before image evaluation, then subsequently reviewed the cases and performed image analysis independently. No data other than the anonymized MRI images were available to the readers.

Using a five-point Likert scale (1–5) (Table 1), readers assessed sharpness of the liver margin, sharpness of intrahepatic vessels, sharpness of the pancreatic duct, homogeneity of fat suppression, strength of fat suppression, in-plane and through-plane motion artifacts, other ghosting artifacts, and overall image quality. In addition, readers evaluated the cases for the presence or absence of focal hepatic lesions, which, if present, were assessed for lesion conspicuity and sharpness of the lesion edge, using the same five-point scale.

Statistical analysis

Acquisition times between traditional T2-FS and DL HASTE-FS were compared using the paired Wilcoxon signed-rank test for each case. Likert scores for each imaging quality metric were tabulated, and descriptive statistics (mean, standard deviation, median, first and third quartiles, and range) were computed for each reader and overall. In addition, the paired Wilcoxon signed-rank test was used to compare imaging quality metrics between sequences. For the subset of cases with focal liver lesions, the corresponding analysis of scores relating to lesion conspicuity and sharpness of lesion edge was performed. Reader score consistency was assessed using intraclass correlation coefficient (ICC) analysis, where < 0.4 = poor agreement, 0.4–0.59 = fair agreement, 0.6–0.74 = good agreement, and 0.75–1 = excellent agreement. All p values were

two sided and considered statistically significant when less than 0.05. Analysis was performed using Microsoft Excel (Microsoft, Redmond, Washington) and MedCalc for Windows (MedCalc Software, Ostend, Belgium).

Prior studies

Recently, a single-shot T2-FS HASTE sequence utilizing deep-learning reconstruction has been employed on clinical 1.5 T MRI liver examinations at our institution, demonstrating decreased imaging times with improved overall image quality [26]. This study utilized a separate patient cohort with MR liver examinations performed at 1.5 T but employed a similar network for image reconstruction and a similar method for reader image analysis.

Statements and declarations

Two authors (DN and SA) are Siemens Healthcare employees, who provided technical assistance, but were not involved in the data acquisition or evaluation, nor did they have direct control of the data.

Results

Acquisition time

Acquisition time for DL HASTE-FS was 54.93 ± 16.69 s, which was significantly ($p < 0.001$) shorter than the acquisition time for traditional T2-FS (114.00 ± 32.98 s) (Table 2).

Image quality and artifact assessment

The results of the subjective assessment of image quality for the DL HASTE-FS and traditional T2-FS sequences by the three readers using the five-point Likert scale are described in Table 3. DL HASTE-FS received significantly higher scores than standard T2-FS for sharpness of liver margin (mean 4.3 vs 3.3; $p < 0.001$), hepatic vessel margin (4.2 vs 3.3; $p < 0.001$), pancreatic duct margin (4.0 vs 1.9; $p < 0.001$); in-plane (4.0 vs 3.2; $p < 0.001$) and through-plane (3.9 vs 3.4; $p < 0.001$) motion artifacts; other ghosting artifacts (4.3 vs 2.9; $p < 0.001$); and overall image quality (4.0 vs 2.9; $p < 0.001$), in addition to receiving a higher score for homogeneity of fat suppression (3.7 vs 3.4; $p = 0.04$) and liver-fat contrast ($p = 0.03$), without receiving a significant difference in scores for strength of fat suppression ($p = 0.22$). A comparison of example cases between T2-FS and DL HASTE-FS is provided in Fig. 1.

Focal liver lesions

A total of 12 focal liver lesions were seen by each reader on both sequences, with the individual reader breakdown as follows: 16 lesions on DL HASTE-FS and 15 on T2-FS for reader 1, 15 lesions on DL HASTE-FS and 12 on T2-FS for reader 2, and 20 lesions on DL HASTE-FS, and 20 on T2-FS for reader 3. For lesions seen by each reader on both sequences, DL HASTE-FS received a significantly higher score than standard T2-FS for sharpness of lesion margin (4.4 vs 3.7; $p = 0.03$), without receiving a significant difference in scores for liver-lesion contrast ($p = 0.68$) (Table 4).

Table 1 Likert scale scoring (1–5) for each imaging quality measure

Imaging quality measure	Scoring system
Overall image quality	1 = Unacceptable, 2 = Poor, 3 = Fair, 4 = Good, 5 = Excellent
Liver edge sharpness and Hepatic vessel clarity	1 = Unacceptable, 2 = Poor (Extreme Blur), 3 = Fair (Moderate Blur), 4 = Good (Mild Blur), 5 = Excellent (No Blur)
Homogeneity and strength of fat suppression	1 = Unacceptable, 2 = Poor, 3 = Fair, 4 = Good, 5 = Excellent
In-plane and through-plane respiratory motion	1 = Unacceptable, 2 = Poor (Extreme Blur), 3 = Fair (Moderate Blur), 4 = Good (Mild Blur), 5 = Excellent (No Blur)
Other ghosting artifacts	1 = Unacceptable, 2 = Poor (Extreme Blur), 3 = Fair (Moderate Blur), 4 = Good (Mild Blur), 5 = Excellent (No Blur)
Sharpness of pancreatic duct Margin	1 = Unacceptable, 2 = Poor (Extreme Blur), 3 = Fair (Moderate Blur), 4 = Good (Mild Blur), 5 = Excellent (No Blur)
Lesion conspicuity	1 = Unacceptable, 2 = Poor, 3 = Fair, 4 = Good, 5 = Excellent
Lesion edge sharpness	1 = Unacceptable, 2 = Poor (Extreme Blur), 3 = Fair (Moderate Blur), 4 = Good (Mild Blur), 5 = Excellent (No Blur)

Table 2 Acquisition time comparison between DL HASTE-FS and T2-FS

Case Number	DL HASTE-FS (seconds)	T2-FS (seconds)	Difference (seconds)
1	26	98	72
2	73	144	71
3	73	104	31
4	67	86	19
5	46	93	47
6	37	55	18
7	58	74	16
8	64	81	17
9	58	95	37
10	29	119	90
11	38	105	67
12	75	165	90
13	60	110	50
14	60	101	41
15	25	87	62
16	60	107	47
17	76	108	32
18	40	98	58
19	67	113	46
20	72	105	33
21	61	110	49
22	56	104	48
23	79	121	42
24	72	153	81
25	55	122	67
26	58	118	60
27	60	105	45
28	63	127	64
29	60	142	82
30	31	62	31
31	32	151	119
32	68	155	87
33	47	106	59
34	46	160	114
35	54	182	128
36	59	107	48
37	33	114	81
38	91	225	134
39	29	81	52
40	27	62	35
41	67	119	52

Inter-reader agreement

Intra-class correlation coefficient (ICC) among the three readers for the overall image quality was fair for DL HASTE-FS (ICC = 0.51, range = 0.31–0.69) and good for T2-FS (ICC = 0.60, range = 0.53–0.70).

Discussion

In our study, DL HASTE-FS received significantly higher scores than standard T2-FS for sharpness of liver margin, hepatic vessel margin, pancreatic duct margin; in-plane and through-plane motion artifacts; other ghosting artifacts; and overall image quality, in addition to receiving a higher score for homogeneity of fat suppression and liver-fat contrast. Strength of fat suppression was comparable for both DL HASTE-FS and T2-FS. For lesions seen by each reader on both sequences, DL HASTE-FS received significantly higher scores than standard T2-FS for sharpness of lesion margin, with comparable scores for liver-lesion contrast. The total acquisition time for the DL HASTE-FS sequence was significantly less than the conventional T2-FS sequence. These results are similar to results seen at 1.5 T utilizing a similar sequence, which demonstrates the generalizability of deep-learning applications across different magnetic field strengths.

Our novel single-shot T2-weighted MRI with deep-learning-based image reconstruction used regular under-sampling without integrated reference data to shorten the echo train duration for the image data and to lower the specific absorption rate, instead acquiring reference data right after the image data with a lower flip angle. In addition, the approach utilized pre-iterations with trainable extrapolations and gradient steps to allow for data reconstruction with an undersampled k-space center. In order to apply the homodyne filter on the network predictions, the network reconstructed complex-value images.

Not only does MRI provide significant information about the background liver parenchyma, biliary tree, and hepatic vasculature, but it often allows for the definitive characterization of various solid and cystic hepatic lesions. Traditional T2-FS images of the liver are essential for this purpose but require a long scan time and often can be wrought with motion artifacts. Even with breath-hold techniques, respiratory motion artifacts often prompt repeat sequence acquisition, increasing overall scan time, and therefore, decreasing patient throughput. Previously, modified acquisition techniques, such as 3D fast spin-echo pulse sequences and periodically rotating overlapping parallel lines with enhanced reconstruction, have been employed to mitigate this and have demonstrated improved overall image quality, but at the cost of increased overall

Table 3 Image quality mean (±SD) score comparison between DL HASTE-FS and T2-FS

Imaging quality measure	Reader 1			Reader 2			Reader 3			Overall		
	DL HASTE-FS	T2-FS	p	DL HASTE-FS	T2-FS	p	DL HASTE-FS	T2-FS	p	DL HASTE-FS	T2-FS	p
Homogeneity of fat suppression	4.05±0.82	3.88±0.67	.31	3.44±1.29	3.15±0.98	.33	3.63±1.05	3.17±0.62	.02	3.71±0.86	3.40±0.48	.04
Strength of fat suppression	4.44±1.04	4.51±0.86	.27	3.61±1.19	3.66±0.98	.14	4.44±1.27	4.56±0.88	.23	4.16±1.07	4.24±0.74	.22
Sharpness of liver margin	4.71±0.45	4.24±0.73	.1	3.66±0.81	2.39±0.73	<.001	4.49±0.59	3.37±0.62	<.001	4.28±0.46	3.33±0.58	<.001
Sharpness of hepatic vessel Margin	4.54±0.59	4.07±0.81	.26	3.54±0.89	2.37±0.79	<.001	4.51±0.59	3.41±0.91	<.001	4.20±0.49	3.28±0.65	<.001
In-plane motion artifact	4.20±0.67	3.51±0.77	.005	3.93±0.89	2.71±0.74	<.001	3.93±0.68	3.44±0.73	<.03	4.02±0.59	3.22±0.54	<.001
Through-plane Motion artifact	4.39±0.76	3.39±0.76	<.001	3.78±0.68	2.63±0.85	<.001	3.63±0.85	4.10±0.66	.005	3.93±0.53	3.37±0.46	<.001
Other ghosting Artifact	4.85±0.42	3.46±0.67	<.001	3.76±0.93	2.41±0.91	<.001	4.37±0.69	2.68±0.90	<.001	4.33±0.51	2.85±0.65	<.001
sharpness of Pancreatic duct	4.20±1.15	1.44±0.88	<.001	3.71±1.06	1.78±0.90	<.001	3.95±0.79	2.51±0.83	<.001	3.95±0.89	1.91±0.75	<.001
liver-fat contrast	0.41±0.41	0.29±0.34	.04	0.38±0.44	0.34±0.32	.06	0.51±0.34	0.46±0.26	.02	0.44±0.35	0.36±0.27	.03
Overall image quality	4.12±0.71	3.41±0.70	.005	3.51±0.80	2.22±0.68	.005	4.29±0.83	3.10±0.88	<.001	3.98±0.64	2.91±0.65	<.001

acquisition times. Alternatively, single-shot T2 FSE has been used to increase motion robustness but demonstrates increased overall image noise, decreased signal-to-noise ratio (SNR) of the liver, and decreased liver-lesion contrast-to-noise ratio (CNR) when compared with traditional T2 FSE, limiting the clinical utility of the technique [31]. Deep-learning (DL) techniques have demonstrated the ability to improve image quality by identifying and mitigating artifacts in accelerated acquisitions, allowing for reduced overall imaging time [23]. This novel single-shot T2-weighted MRI with deep-learning-based image reconstruction sequence offers a potential solution to these previously encountered issues.

One limitation of our study was the number of patients included, which was limited by the number of patients receiving both traditional T2-FS and DL HASTE-FS sequences at the time of the study. Although the results of this study are promising for future clinical application of the sequence, and potential replacement of the traditional T2-FS sequence at our institution, a larger study will be required to compare the two sequences' utility in lesion detection and characterization. Additionally, only outpatients were included in this study due to the limited availability of the prototype sequence on two MRI systems at an outpatient facility. Finally, we did not analyze the discrepancy in lesions detection rate both between readers for each sequence and for the first two readers between sequences. The discrepancy between readers on each sequence may have been secondary to each author's interpretation of what constitutes a notable lesion. However, for readers 1 and 2, more lesions were seen on DL HASTE-FS than on T2-FS, for which the clinical significance of this discrepancy is unclear and beyond the scope of this study.

In conclusion, our novel single-shot T2-weighted MRI with deep-learning-based image reconstruction demonstrated superior image quality compared with the standard T2-FS sequence for routine clinical liver MRI at 3 T, while being acquired in less than half the time. Therefore, DL HASTE-FS is a potential alternative to traditional T2-FS in routine clinical liver MRI.

Table 4 Overall image quality mean (±SD) score comparison between DL HASTE-FS and T2-FS for focal lesions seen by each reader on both sequences (N = 12)

Imaging quality measure	Overall		
	DL HASTE-FS	T2-FS	p
Lesion conspicuity	4.64±0.63	4.39±0.83	.45
Sharpness of lesion margin	4.43±0.55	3.71±0.92	.03
Liver-lesion contrast	0.47±0.23	0.55±0.26	.68

Case	29	34	36
T2-FS			
DL HASTE-FS			

Fig. 1 Example cases comparison between T2-FS and DL HASTE-FS

Declarations

References

1. Helmberger TK, Schröder J, Holzknecht N, et al. T2-weighted breathold imaging of the liver: a quantitative and qualitative comparison of fast spin echo and half Fourier single shot fast spin echo imaging. *Magma (New York, NY).* 1999;9(1-2):42-51.
2. Jiang HY, Chen J, Xia CC, Cao LK, Duan T, Song B. Noninvasive imaging of hepatocellular carcinoma: From diagnosis to prognosis. *World journal of gastroenterology.* 2018;24(22):2348-2362.
3. Su Q, Bi S, Yang X. Prioritization of liver MRI for distinguishing focal lesions. *Science China Life sciences.* 2017;60(1):28-36.
4. Donato H, França M, Candelária I, Caseiro-Alves F. Liver MRI: From basic protocol to advanced techniques. *European journal of radiology.* 2017;93:30-39.
5. Rydberg JN, Lomas DJ, Coakley KJ, Hough DM, Ehman RL, Riederer SJ. Comparison of breath-hold fast spin-echo and conventional spin-echo pulse sequences for T2-weighted MR imaging of liver lesions. *Radiology.* 1995;194(2):431-437.
6. Reinig JW. Breath-hold fast spin-echo MR imaging of the liver: a technique for high-quality T2-weighted images. *Radiology.* 1995;194(2):303-304.
7. McFarland EG, Mayo-Smith WW, Saini S, Hahn PF, Goldberg MA, Lee MJ. Hepatic hemangiomas and malignant tumors: improved differentiation with heavily T2-weighted conventional spin-echo MR imaging. *Radiology.* 1994;193(1):43-47.
8. Ito K, Mitchell DG, Outwater EK, Szklaruk J, Sadek AG. Hepatic lesions: discrimination of nonsolid, benign lesions from solid, malignant lesions with heavily T2-weighted fast spin-echo MR imaging. *Radiology.* 1997;204(3):729-737.
9. Outwater EK, Mitchell DG, Vinitski S. Abdominal MR imaging: evaluation of a fast spin-echo sequence. *Radiology.* 1994;190(2):425-429.
10. Siegelman ES, Outwater EK. MR imaging techniques of the liver. *Radiologic clinics of North America.* 1998;36(2):263-286.
11. Ichikawa T, Araki T. Fast magnetic resonance imaging of liver. *European journal of radiology.* 1999;29(3):186-210.
12. Schreiber-Zinaman J, Rosenkrantz AB. Frequency and reasons for extra sequences in clinical abdominal MRI examinations. *Abdominal radiology (New York).* 2017;42(1):306-311.
13. Rosenkrantz AB, Mannelli L, Mossa D, Babb JS. Breath-hold T2-weighted MRI of the liver at 3T using the BLADE technique: impact upon image quality and lesion detection. *Clinical radiology.* 2011;66(5):426-433.
14. Rosenkrantz AB, Patel JM, Babb JS, Storey P, Hecht EM. Liver MRI at 3 T using a respiratory-triggered time-efficient 3D T2-weighted technique: impact on artifacts and image quality. *AJR American journal of roentgenology.* 2010;194(3):634-641.
15. Keogan MT, Spritzer CE, Paulson EK, et al. Liver MR imaging: comparison of respiratory triggered fast spin echo with

T2-weighted spin-echo and inversion recovery. *Abdominal imaging.* 1996;21(5):433-439.

16. Coates GG, Borrello JA, McFarland EG, Mirowitz SA, Brown JJ. Hepatic T2-weighted MRI: a prospective comparison of sequences, including breath-hold, half-Fourier turbo spin echo (HASTE). *Journal of magnetic resonance imaging : JMRI.* 1998;8(3):642-649.

17. Yu JS, Kim KW, Kim YH, Jeong EK, Chien D. Comparison of multishot turbo spin echo and HASTE sequences for T2-weighted MRI of liver lesions. *Journal of magnetic resonance imaging : JMRI.* 1998;8(5):1079-1084.

18. Tang Y, Yamashita Y, Namimoto T, Abe Y, Takahashi M. Liver T2-weighted MR imaging: comparison of fast and conventional half-Fourier single-shot turbo spin-echo, breath-hold turbo spin-echo, and respiratory-triggered turbo spin-echo sequences. *Radiology.* 1997;203(3):766-772.

19. Lee SS, Byun JH, Hong HS, et al. Image quality and focal lesion detection on T2-weighted MR imaging of the liver: comparison of two high-resolution free-breathing imaging techniques with two breath-hold imaging techniques. *Journal of magnetic resonance imaging : JMRI.* 2007;26(2):323-330.

20. Kim BS, Kim JH, Choi GM, et al. Comparison of three free-breathing T2-weighted MRI sequences in the evaluation of focal liver lesions. *AJR American journal of roentgenology.* 2008;190(1):W19-27.

21. Reimer P, Rummeny EJ, Wissing M, Bongartz GM, Schuierer G, Peters PE. Hepatic MR imaging: comparison of RARE derived sequences with conventional sequences for detection and characterization of focal liver lesions. *Abdominal imaging.* 1996;21(5):427-432.

22. Hammernik K, Klatzer T, Kobler E, et al. Learning a variational network for reconstruction of accelerated MRI data. *Magnetic resonance in medicine.* 2018;79(6):3055-3071.

23. Chen F, Taviani V, Malkiel I, et al. Variable-Density Single-Shot Fast Spin-Echo MRI with Deep Learning Reconstruction by Using Variational Networks. *Radiology.* 2018;289(2):366-373.

24. Schlemper J, Caballero J, Hajnal JV, Price AN, Rueckert D. A Deep Cascade of Convolutional Neural Networks for Dynamic MR Image Reconstruction. *IEEE transactions on medical imaging.* 2018;37(2):491-503.

25. Qin C, Schlemper J, Caballero J, Price AN, Hajnal JV, Rueckert D. Convolutional Recurrent Neural Networks for Dynamic MR Image Reconstruction. *IEEE transactions on medical imaging.* 2019;38(1):280-290.

26. Shanbhogue K, Tong A, Smereka P, et al. Accelerated single-shot T2-weighted fat-suppressed (FS) MRI of the liver with deep learning-based image reconstruction: qualitative and quantitative comparison of image quality with conventional T2-weighted FS sequence. *European radiology.* 2021.

27. Laader A, Beiderwellen K, Kraff O, et al. 1.5 versus 3 versus 7 Tesla in abdominal MRI: A comparative study. *PloS one.* 2017;12(11):e0187528.

28. Kuhl CK, Träber F, Schild HH. Whole-body high-field-strength (3.0-T) MR Imaging in Clinical Practice. Part I. Technical considerations and clinical applications. *Radiology.* 2008;246(3):675–696.

29. Lauenstein TC, Sharma P, Hughes T, Heberlein K, Tudorascu D, Martin DR. Evaluation of optimized inversion-recovery fat-suppression techniques for T2-weighted abdominal MR imaging. *Journal of magnetic resonance imaging : JMRI.* 2008;27(6):1448-1454.

30. Parrish T, Hu X. A new T2 preparation technique for ultra-fast gradient-echo sequence. *Magnetic resonance in medicine.* 1994;32(5):652-657.

31. Klessen C, Asbach P, Kroencke TJ, et al. Magnetic resonance imaging of the upper abdomen using a free-breathing T2-weighted turbo spin echo sequence with navigator triggered prospective acquisition correction. *Journal of magnetic resonance imaging : JMRI.* 2005;21(5):576-582.